Analytical and numerical study of particles with binary adsorption

C. S. Dias,[1,*] N. A. M. Araújo,[2,†] and A. Cadilhe[3,‡]
[1]*GCEP-Centro de Física da Universidade do Minho, 4710-057 Braga, Portugal*
[2]*Computational Physics for Engineering Materials, IfB, ETH Zürich, Schafmattstr. 6, CH-8093 Zürich, Switzerland*
[3]*Theoretical Division, MSK 717, Los Alamos National Laboratory, Los Alamos, New Mexico 87545, USA*
(Received 27 February 2012; published 13 April 2012)

Electro-oxidation of ethanol represents a key process in fuel-cell technology. We introduce a generalization of the random sequential adsorption model to study the long time scale and large length scale properties of the electro-oxidation process. We provide an analytical solution for one dimension and Monte Carlo results in two dimensions. We characterize the coverage and percolation properties of the jammed state and unveil the influence of quenched impurities in the selectivity of oxidation products.

DOI: 10.1103/PhysRevE.85.041120 PACS number(s): 02.50.Ey, 68.43.De

I. INTRODUCTION

Ethanol has been considered for fuel cells, given its low toxicity and abundance [1]. The electro-oxidation of ethanol on the surface of catalysts can follow multiple reaction pathways leading to several different products, which are strongly affected by, e.g., concentration, presence of impurities, and temperature. In this work, we introduce a model, inspired by the random sequential adsorption (RSA) model of dimers, to analyze properties of the oxidation process such as their dependence on the binding configuration, binding rates, and reaction pathway probabilities.

Ethanol electro-oxidation has recently been studied through density function theory [2,3], providing possible reaction pathways for the adsorption and catalysis of ethanol. However, the time dependence of the coverage based on the various reaction pathways would become computationally prohibitive using density functional theory. Nonetheless, in the limit of low mobility of bound reaction products, large systems sizes, and long time scales, a study based on the adoption of a square lattice to represent the (100) substrate for the various reaction products becomes appropriate. In this limit, ethanol electro-oxidation can be described as adsorption of a dimer on the substrate, thus occupying two adjacent lattice sites, as it cleaves [2,3] or, in the presence of neighboring preadsorbed species, is adsorbed as a monomer. A key feature of the model is to provide a configuration-dependent rule for the landing site and study the influence on the adsorption rates of the oxidation process. We also study the influence of immobile impurities and clarify their role in achieving selectivity of adsorbed species. Our model can also be extended to analyze other cleavage mechanisms, e.g., that of sugars [4].

The RSA model has been utilized to describe adsorption in the limit of low surface mobility and of negligible desorption rate [5–14]. Adsorption attempts occur sequentially at randomly selected sites, where particles interact solely through excluded volume. Generalized versions have been proposed where the rates of adsorption are dependent on the local configuration [5,15], which might, e.g., explain the selectivity of adsorbed species [16]. Further extensions have been considered to study a wide range of problems, such as chemical reactions [17–19], adsorption on membranes [20], and protein and colloid adsorption [21,22] with and without preadsorbed impurities [23–28].

In this paper, we study the model above delineated in both one and two dimensions. In the one-dimensional study, we were able to establish a closed hierarchy of rate equations for which we could obtain exact, closed-form solutions. To complement and extend the insight provided by this approach, we also performed a Monte Carlo (MC)–based study for the relevant two-dimensional case.

The paper is organized as follows: in the next section we introduce the model, while in Sec. III an analytical derivation is exactly solved in three specific limits. MC simulations extend the one-dimensional results to the more realistic case of a substrate as described in Sec. IV, with results provided in Sec. V for substrates with and without impurities. Final remarks are presented in Sec. VI.

II. MODEL

Ethanol oxidation is of great relevance to society, since each molecule releases twice as much energy as one methanol molecule [29], posing it as a candidate to replace several sources of energy [30]. Recently, Wang and Liu [2] proposed a mechanism for ethanol electro-oxidation on Pt(100) and Pt(111) substrates, which can be summarized in three pathways [3]:

(1) The *OH path*, where the cleavage of the hydroxyl group leads to the formation of acetaldehyde, which is then adsorbed.

(2) The *CH path*, where CH_3CHOH is an intermediate product that degrades into CH_3COH.

(3) The *concerted path* where the ethanol molecule loses two hydrogens, followed by the desorption of acetaldehyde.

Wang and Liu have shown that for the Pt(100) surface (which can be mapped onto a square lattice), the relevant pathway is mainly the CH path [2], where ethanol adsorption leads to the formation of acetyl (CH_3CO). The work of Wang and Liu [2] discloses that the adsorption mechanism is strongly influenced by the actual surface coverage. At low surface coverages, the acetyl dehydrogenates into CH_2CO or CHCO, which leads to a C-C bond cleavage, yielding CH and CO fragments. Under oxidative conditions, both fragments react

*cristovao@fisica.uminho.pt
†nuno@ethz.ch
‡cadilhe@lanl.gov

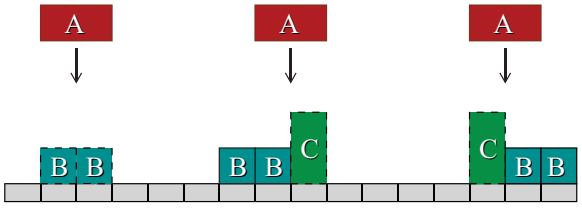

FIG. 1. (Color online) Schematic representation of the adsorption rules (1). The A species (red) can deposit either as dimers, on two empty sites, yielding B products (blue), or as monomers, on one empty site with at least one occupied neighbor, yielding C products (green). In ethanol oxidation, A is the ethanol, B stands for the two products (CH and CO), and C the acetyl.

with the oxygen, O, present on the surface and desorb as carbon dioxide CO_2. Desorption of cleaved products can be neglected for nonoxidative conditions, which leads to a jammed state, whereas when the surface coverage is high, the C-C bond cleavage is blocked, and the surface becomes poisoned by acetyl.

Based on the proposed mechanism, we introduce a model which can be summarized by the rules

$$\begin{aligned} A + 2v &\xrightarrow{k_d} 2B, \\ A + v &\xrightarrow{k_m} C, \end{aligned} \tag{1}$$

where A represents ethanol, v an empty site, $2B$ represents cleaved products, C is acetyl, and k_d (k_m) stands for dimer (monomer) production rates. Note that, as discussed below, adsorption as a monomer (with product C) can only occur in the neighborhood of an occupied site.

As sketched in Fig. 1, dimers are uniformly formed on the substrate (lattice). Successful adsorption of dimers requires two neighboring empty sites. If only one is available, the species adsorbs as a monomer. When both sites are occupied, due to the excluded volume interaction, the adsorption attempt fails and the particle attempting adsorption is no longer considered. The model differs from traditional cooperative sequential adsorption models [5] since, for the latter, the rates of adsorption depend on the state of the nearest neighbors but not, as in the present model, on the occupation of the local configuration provided by neighboring adsorbed sites. Despite the focus on the electro-oxidation of ethanol, the model could be utilized for the study of any other process dependent on the local configuration rather than on constant, configuration-independent, deposition rates.

III. ANALYTICAL STUDY

The time dependence of the coverage and distribution of empty sites can be analytically obtained by establishing a closed hierarchy of rate equations as explained below. To account for the different rates for monomer and dimer adsorption [see Eq. (1)], we consider a competitive deposition of monomers and dimers, with different deposition rates (k_m and k_d, respectively), under the constraint that monomers can only deposit in the neighborhood of occupied sites. Results are divided into three limiting cases: equal rates for dimers and monomers (Sec. III A), preferential dimer site adsorption (Sec. III B), and different deposition rates for monomers and dimers (Sec. III C).

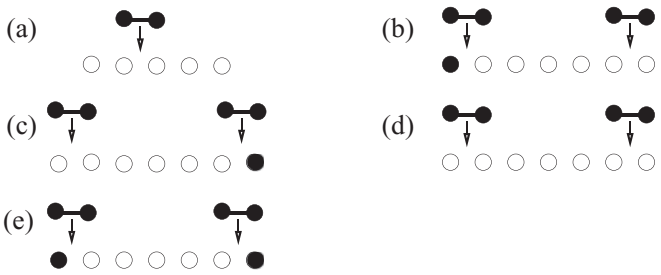

FIG. 2. Catalog of possible adsorption attempts of a dimer on a segment of empty sites with length $n = 5$, which is part of a larger segment of length ℓ ($\ell \geqslant n$). For adsorption events with both landing sites in segment n, a dimer is adsorbed (a). For adsorption events with a single landing site in the n segment, either a dimer or a monomer is adsorbed, depending on the occupation state of the neighboring site (b–e).

Let us start by considering a segment of empty sites of size n which is part of a larger (or equal) one with size $\ell \geqslant n$. Since the neighboring sites of this segment are not necessarily occupied, the possible adsorption events depend on the configuration of the neighbors. A segment can be reduced in size by adsorption of a monomer on the left-hand side of the segment [Fig. 2(b)], on the right-hand side [Fig. 2(c)], or on both sides [Fig. 2(e)]. It can also be split (or reduced in size) by the adsorption of a dimer on any site of the segment [Fig. 2(a)], the right-hand side [Fig. 2(b)], the left-hand side [Fig. 2(c)], or both sides [Fig. 2(d)].

We define P_n as the probability that a randomly selected site belongs to any segment n defined before. Each configuration of the catalog in Fig. 2 is obtained with a probability $P[\cdots]$ given by

$$\begin{aligned} P[\circ\circ\circ\circ\circ] &= P_n, \\ P[\bullet\circ\circ\circ\circ\circ\circ] &= P[\circ\circ\circ\circ\circ\circ\bullet] = P_{n+1} - P_{n+2}, \\ P[\circ\circ\circ\circ\circ\circ\circ] &= P_{n+2}, \\ P[\bullet\circ\circ\circ\circ\circ\bullet] &= 2P_n - 2P[\bullet\circ\circ\circ\circ\circ\circ] - P[\circ\circ\circ\circ\circ\circ\circ] \\ &= P_n - 2P_{n+1} + P_{n+2}. \end{aligned} \tag{2}$$

The proper set of rate equations depends on the case. Below, we describe this set for equal rates of dimers and monomers, adsorption of a preferential dimer site, and different rates for dimers and monomers.

A. Equal deposition rate of dimers and monomers

For equal deposition rates of monomers and dimers, the rate of both species is considered as k. Since P_n refers to the probability that a randomly selected site belongs to any segment of n empty sites, which can be part of a larger one, this probability can never increase with time. The rate of change of P_n due to the adsorption of dimers is given by

$$\begin{aligned} (\dot{P}_n)_d &= -k(n-1)P_n - kP[\bullet\circ\circ\circ\circ\circ\circ] \\ &\quad - kP[\circ\circ\circ\circ\circ\circ\bullet] - 2kP[\circ\circ\circ\circ\circ\circ\circ] \\ &= -(n-1)kP_n - 2kP_{n+1}, \end{aligned} \tag{3}$$

where $(n-1)$ corresponds to the destruction rate of a segment with, at least, n empty sites, which is 0 for $n=1$ [see Fig. 2(a)]. The rate of change due to monomer adsorption is

$$(\dot{P}_n)_m = -2kP[\bullet\circ\circ\circ\circ\circ\bullet] - kP[\bullet\circ\circ\circ\circ\circ\circ] - kP[\circ\circ\circ\circ\circ\circ\bullet] = -2k(P_n - P_{n+1}). \quad (4)$$

From Eqs. (3) and (4), the total rate of change is given by

$$(\dot{P}_n)_T = (\dot{P}_n)_d + (\dot{P}_n)_m = -(n+1)kP_n. \quad (5)$$

This result is equivalent to considering that, regardless of the type of adsorption, a segment of n, or more, empty sites can be destroyed by adsorption on $(n+1)$ different places. This equation gives $P_n(t) = \exp[-(n+1)kt]$. The coverage θ can then be obtained from the probability that a certain site is part of a segment of size $n \geqslant 1$, i.e.,

$$\theta(t) = 1 - P_1(t) = 1 - \exp(-2kt). \quad (6)$$

Defining $s_m(n)$ as the rate of monomer adsorption on an n segment, i.e., $s_m(n) = -(\dot{P}_n)_m$, we obtain

$$s_m(n) = 2k(P_n - P_{n+1}) = 2k[\exp(-[n+1]kt) - \exp(-[n+2]kt)]. \quad (7)$$

The adsorption of monomers on a segment of size $n \geqslant 1$, is given by,

$$s_m(n=1) = 2k[\exp(-2kt) - \exp(-3kt)]. \quad (8)$$

From the rate of adsorption, the coverage of monomers can be obtained from $\dot{\theta}_m = s_m$ for $n=1$, giving

$$\theta_m(t) = [1 - \exp(-2kt)] + \tfrac{2}{3}[\exp(-3kt) - 1]. \quad (9)$$

Now defining $s_d(n)$ as the rate of dimer adsorption on an n segment, i.e., $s_d(n) = -(\dot{P}_n)_d$, we obtain

$$s_d(n) = k[(n-1)\exp(-[n+1]kt) + 2\exp(-[n+2]kt)]. \quad (10)$$

The adsorption of dimers on a segment of size $n \geqslant 1$ is then given by

$$s_d(n=1) = 2k\exp(-3kt). \quad (11)$$

Knowing the rate of adsorption, the coverage of dimers can be obtained from the rate equation, $\dot{\theta}_d = s_d(n=1)$,

$$\theta_d(t) = \tfrac{2}{3}[1 - \exp(-3kt)]. \quad (12)$$

B. Adsorption of a preferential dimer site

Considering a preferential dimer site means that the symmetry is broken and the first adsorption on the substrate occurs through a specific compound of the dimer. The cleavage only takes place if there is a neighboring empty site, in any direction, to adsorb the other compound. In one dimension, the left site of the dimer is considered to be the preferred one. By symmetry, results are independent of the considered one. For this special case, the change in the P_n by dimers is

$$(\dot{P}_n)_d = -k(n-1)P_n - kP[\bullet\circ\circ\circ\circ\circ\circ] - kP[\circ\circ\circ\circ\circ\circ\bullet] - 2kP[\circ\circ\circ\circ\circ\circ\circ] = -(n-1)kP_n - 2kP_{n+1}, \quad (13)$$

while that by monomers is

$$(\dot{P}_n)_m = -kP[\bullet\circ\circ\circ\circ\circ\bullet] - kP[\circ\circ\circ\circ\circ\circ\bullet] = -k(P_n - P_{n+1}). \quad (14)$$

For the total change in P_n we obtain

$$(\dot{P}_n)_T = (\dot{P}_n)_d + (\dot{P}_n)_m = -nkP_n - kP_{n+1}. \quad (15)$$

Considering the relation between P_n and P_{n+1} as $P_{n+1} = Q_nP_n$ [31], then

$$\dot{P}_{n+1} = -(n+1)kQ_nP_n - kQ_{n+1}Q_nP_n, \quad (16)$$

and plugging it back into Eq. (15), we obtain

$$\frac{dQ_n}{dt}\frac{1}{Q_n} = -(n+1)k + nk - k(Q_{n+1} - Q_n). \quad (17)$$

If we assume $Q_{n+1} = Q_n$, then $\frac{dQ_n}{Q_n} = -kdt$. Therefore, $Q_n(t) = \exp(-kt)$, which, when replaced in Eq. (17), gives $\dot{P}_n = -[nk + k\exp(-kt)]P_n$, and so,

$$P_n(t) = \exp[-nkt + (\exp[-kt] - 1)]. \quad (18)$$

Since the coverage θ is dependent on the evolution of the probability of finding a segment of size $n \geqslant 1$,

$$\theta(t) = 1 - P_1(t) = 1 - \exp[-kt + (\exp[-kt] - 1)]. \quad (19)$$

The independent rates of adsorption for dimers and monomers and the subsequent calculation of the coverage for each species are obtained as before.

C. Different deposition rates for dimers and monomers

To attempt a generic solution for the rules given by Eq. (1), it is necessary to consider different deposition rates for monomers (k_m) and dimers (k_d). Accounting for the rate of change of P_n by dimers given by Eq. (3),

$$(\dot{P}_n)_d = -(n-1)k_dP_n - 2k_dP_{n+1}, \quad (20)$$

while accounting for that by monomers,

$$(\dot{P}_n)_m = -2k_m(P_n - P_{n+1}). \quad (21)$$

The change in the the total P_n over time is then given by

$$(\dot{P}_n)_T = (\dot{P}_n)_d + (\dot{P}_n)_m = -[k_d(n-1) + 2k_m]P_n - 2(k_d - k_m)P_{n+1}. \quad (22)$$

For the sake of simplicity, we define $\alpha_n = (n-1)k_d + 2k_m$ and $\beta = k_d - k_m$. In the same way as before, applying the relation $P_{n+1} = Q_nP_n$, the rate equation for P_{n+1} is

$$\dot{P}_{n+1} = \dot{Q}_nP_n + Q_n\dot{P}_n = -\alpha_{n+1}Q_nP_n - 2\beta Q_{n+1}Q_nP_n, \quad (23)$$

and replacing $\dot{P}_n$ by Eq. (21),

$$\dot{Q}_nP_n + Q_n[-(\alpha_n + 2\beta Q_n)P_n] = -(\alpha_{n+1}Q_n + 2\beta Q_{n+1}Q_n)P_n, \quad \dot{Q}_n = -k_dQ_n - 2\beta(Q_{n+1} - Q_n)Q_n. \quad (24)$$

Considering $Q_{n+1} = Q_n$, then $Q_n(t) = \exp(-k_dt)$. From the above result, Eq. (22) simplifies as $\dot{P}_n = -(\alpha_n - 2\beta Q_n)P_n$,

which gives

$$P_n(t) = \exp\Big[-([n-1]k_d + 2k_m)t - \frac{2(k_d - k_m)}{k_d}(1 - \exp[-k_d t])\Big]. \quad (25)$$

From Eq. (6),

$$\theta(t) = 1 - P_1(t) = 1 - \exp\left[-2k_m t - \frac{2(k_d - k_m)}{k_d}(1 - \exp[-k_d t])\right], \quad (26)$$

which, for $k_m = k_d = k$, boils down to Eq. (6). If $s_m(n)$ is defined as the rate of monomer adsorption on an n segment, $s_m(n) = -(\dot{P}_n)_m$ and so

$$s_m(n) = 2k_m(1 - Q_n)P_n. \quad (27)$$

The relations $y = \exp(-k_d t)$ and $\gamma = \frac{k_m}{k_d}$ are considered and the adsorption of monomers on a segment of size $n \geqslant 1$ is given by

$$s_m(1) = 2k_m(1 - y)y^{2\gamma}\exp[-2(1 - \gamma)(1 - y)]. \quad (28)$$

From the rate of adsorption, the coverage of monomers is given by $\dot{\theta}_m = s_m$ for $n = 1$, and so,

$$\theta_m = -\int_1^{\exp(-k_d t)} s_m(1)(y k_d)^{-1} dy. \quad (29)$$

The dimer rate of adsorption is then

$$s_d(n) = k_d(n - 1)P_n + 2k_d Q_n P_n. \quad (30)$$

For the sake of simplicity, the relation $y = \exp(-t)$ is used, and the adsorption of dimers on a segment of size $n \geqslant 1$ is given by

$$s_d(1) = 2k_d y^{k_d + 2k_m}\exp\left[-\frac{2(k_d - k_m)}{k_d}(1 - y^{k_d})\right]. \quad (31)$$

For the rate of adsorption, the coverage of monomers can be given by $\dot{\theta}_d = s_d$ for $n = 1$, which, by integrating over y, gives

$$\theta_d = -\int_1^{\exp(-t)} s_d(1) y^{-1} dy. \quad (32)$$

IV. ONE-DIMENSIONAL MONTE CARLO SIMULATIONS

We numerically studied the proposed model through MC simulations, performed on a lattice with 10^4 sites, where periodic boundary conditions have been applied and results have been averaged over 10^2 samples.

The coverage as a function of time is plotted in Figs. 3(a)–3(c) for the three previously described cases. The total coverage θ_T, the coverage of dimers θ_d, and the coverage of monomers θ_m are computed over 10 MC sweeps, where one MC sweep corresponds to one adsorption attempt per lattice site. Figure 3(a) shows the case of equal deposition rates for dimers and monomers, where $k_d = k_m = 1$. The solid lines in the plot represent the analytical solution given by Eqs. (6), (9), and (12). The preferential dimer site rule of adsorption is in Fig. 3(b), where, despite the values of the deposition

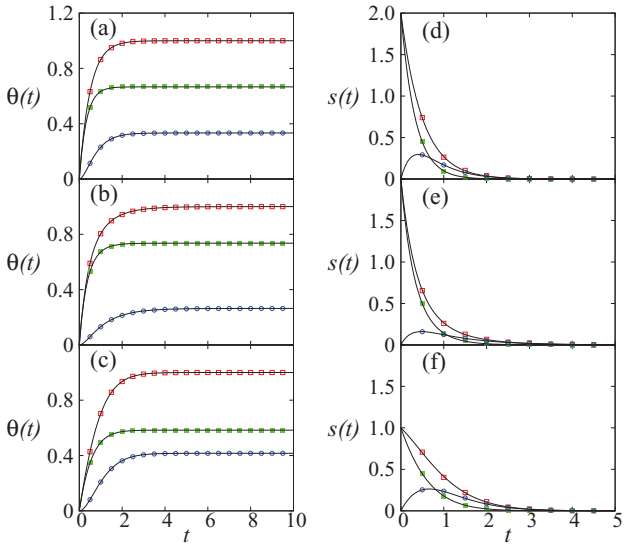

FIG. 3. (Color online) Coverage $\theta(t)$ and rates of adsorption $s(t)$ as a function of time obtained through Monte Carlo simulations (symbols) and analytically (solid line) for equal rates of adsorption (a and d), preferential carbon adsorption (b and e), and different rates of adsorption ($k_d = 0.5$ and $k_m = 1$; c and f). Total coverage and rates of adsorption (open squares), dimers (filled squares), and monomers (open circles).

rates being given by $k_d = k_m = 1$, the results are equivalent to the ones for $k_d = 1$ and $k_m = 0.5$, since the deposition of a monomer by the nonfavored dimer site is not allowed. For these rules of deposition, the exact results are given by Eqs. (19), (13), and (14). The final case, where a different deposition rate for dimers and monomers is considered, is plotted in Fig. 3(c), with deposition rates of $k_d = 0.5$ and $k_m = 1$. The exact solution is given by Eqs. (26), (29), and (32). For all cases, data points from MC lay on the line given by the exact solution.

Figures 3(d)–3(f) show the rates of adsorption as a function of time (only five MC sweeps are shown). Figures 3(d)–3(f) correspond, respectively, to equal deposition rates, preferential dimer site rule, and different deposition rates. Under the same conditions as for the coverage study, some particular aspects can be observed. The dimer rate of adsorption, for instance, starts at a value of 2 for $k_d = 1$ since dimers occupy two sites at each deposition. The monomer rate of adsorption starts at 0 and increases as it requires previously adsorption of, at least, one particle. The rate of monomer adsorption increases due to the large influence of the substrate coverage and reaches a maximum when the number of isolated empty sites start to decrease. Exact results are shown for each plot, consistent with the ones obtained with MC simulations.

Since desorption is neglected, a jamming limit is obtained where no further particles can be adsorbed. In Fig. 4, we see the coverage in the jamming limit θ_∞ as a function of the ratio between dimer and monomer deposition rates, $R = k_d/k_m$, where the solid line is the analytical solution, open circles are dimers, and filled squares are monomers. It can be observed that in the limit of $R \ll 1$, complete coverage of monomers is found, except for one dimer, which always needs to be adsorbed to start the monomer deposition. With the decrease

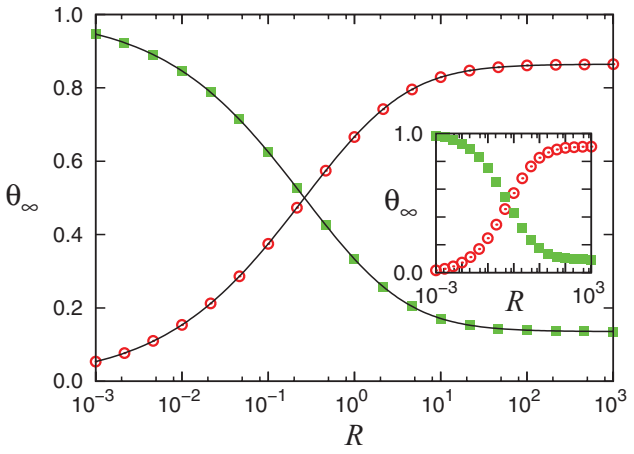

FIG. 4. (Color online) Coverage of dimers (open circles) and monomers (filled squares) for Monte Carlo simulations and obtained analytically (solid line), with the analytical solution (solid line), at the jamming limit as a function of the ratio between the rate of deposition of dimers and monomers R for the one-dimensional case. Inset: Two-dimensional Monte Carlo results.

in the coverage of monomers, an increase in the coverage of dimers is observed, where equal coverage is reached for a ratio $R = 0.207 \pm 0.006$. In the limit of $R \gg 1$, maximum coverage of dimers is obtained, in agreement with the classical adsorption of dimers in a one-dimensional lattice [5]. MC results are also in agreement with the analytical solution.

V. TWO-DIMENSIONAL MONTE CARLO SIMULATIONS

In two dimensions, even for the simplest case of dimer adsorption, no analytical solution has been found. However, it is a case of interest, especially the regular square lattice, which reproduces, for example, the topology of the Pt(100) surface. In this section, we study the proposed model on a square lattice through MC simulations. We devote special attention to the percolation properties of aggregates of monomers and dimers [32].

MC simulations have been performed on square lattices of linear sizes $L = \{128,256,512\}$ in units of lattice sites, with periodic boundary conditions in both directions. Results have been averaged over 10^4 samples. To decrease the computational effort, a rejection-free algorithm was implemented, where the next adsorption trial takes place on an empty site randomly selected from a list of available sites, where the weight of each configuration is properly taken into account. To accurately follow the time evolution, the entire population of events is considered, as well as the rate of monomer and dimer adsorption.

Simulations have been performed on both clean and impurity-covered substrates. Impurities are considered to be quenched and to solely influence the adsorption process by purely geometrical restrictions.

A. Clean substrate

On a clean substrate, the coverage of dimers is larger than the coverage of monomers and the rate of adsorption of monomers as a function of time has a maximum, as also observed in the one-dimensional case. However, the coverage of monomers is favored in two dimensions since each deposited dimer has a greater influence on monomer deposition than in one dimension, mainly due to a larger fraction of configurations with occupied and empty neighboring sites. This can be observed in the inset in Fig. 4, where we plot the jamming limit θ_∞ as a function of the ratio R. In this case, the point of equal coverage for dimers and monomers occurs for a ratio $R \approx 0.6$, which is higher than in one dimension, corroborating that monomers are favored.

The percolation properties are analyzed by identifying clusters with the Hoshen-Kopelman algorithm [33]. While for lower values of R the system is dominated by monomers, as discussed for one dimension, for higher values of R, dimers dominate. Percolation of monomers or dimers is then observed with R as a control parameter. In Fig. 5(a) we plot the

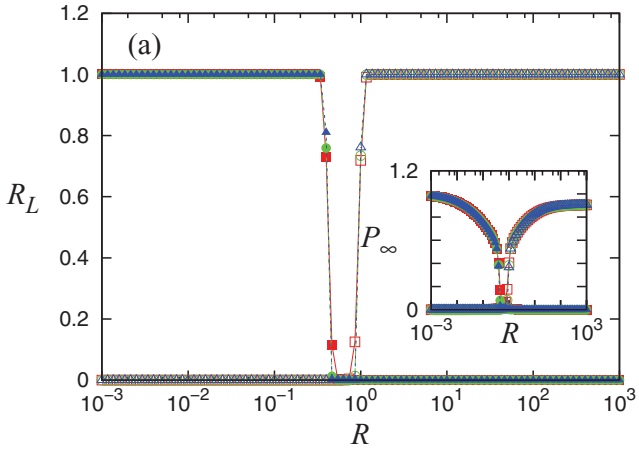

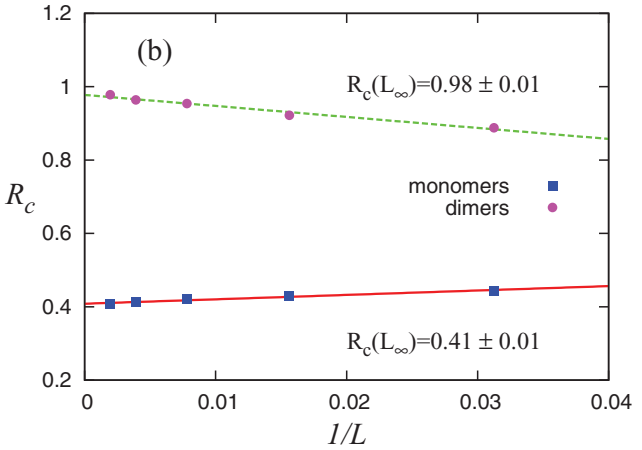

FIG. 5. (Color online) (a) Dependence on the ratio R of the spanning probability R_L for dimers (open) and monomers (filled). Square lattices have been considered with 128^2 (squares), 256^2 (circles), and 512^2 (triangles) lattice sites, for the spanning probability R_L and fraction of sites belonging to the largest cluster P_∞ (inset). (b) Percolation threshold (R_c) as a function of the system sizes, for linear sizes of $L = \{32,64,128,256,512\}$, for dimers (filled circles) and monomers (filled squares).

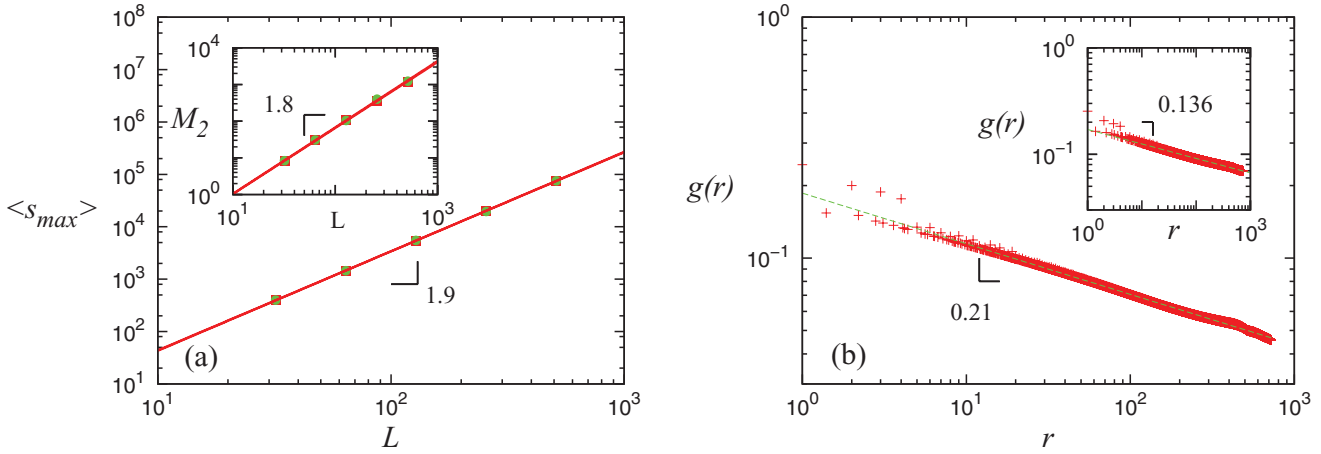

FIG. 6. (Color online) (a) Largest cluster $s_{\max}$ and (inset) second moment of the cluster size distribution function M_2 at R_c as a function of the system sizes, for linear sizes of $L = \{32,64,128,256,512\}$, for dimers (filled circles) and monomers (filled squares). Fractal dimension for monomers and dimers of $D_m = 1.898 \pm 0.008$ and $D_m = 1.890 \pm 0.009$, respectively. (b) Correlation function $g(r)$ for dimers (monomers in the inset) for a system of linear size $L = 1024$ and averaged over 100 samples with a power-law exponent of $\eta = 0.2101 \pm 0.0002$ ($\eta = 0.1361 \pm 0.0002$).

spanning probability R_L defined as the probability of having a percolation cluster touching opposite borders of the lattice. At the percolation transition of both monomers and dimers, the fraction of sites occupied by the species under study is compatible with the percolation threshold for site percolation in the considered topology [34]. The inset in Fig. 5(a) shows the fraction of sites belonging to the largest cluster P_∞ (the order parameter of the percolation transition).

The percolation threshold R_c can be estimated by analyzing the maximum value of the standard deviation of the spanning probability. It can be observed in Fig. 5(b) that the percolation threshold scales linearly with the inverse of the lattice lateral size, L, obtaining $R_c(L_\infty) = 0.98 \pm 0.01$ for dimers and $R_c(L_\infty) = 0.41 \pm 0.01$ for monomers.

The scaling of the average size of the largest cluster $\langle s_{\max} \rangle$ at R_c is in Fig. 6(a) and scales as $\sim L^{D_f}$, where D_f is the fractal dimension. For both monomers and dimers the obtained scaling for the mass of the largest cluster is consistent with the fractal dimension $D_f = 91/48 = 1.8958$ of the classical percolation universality class [34].

Another important parameter to be taken into account is the second momentum of the cluster-size distribution, given by

$$M_2 = \frac{\sum_{i \neq \max} s_i^2}{N}, \tag{33}$$

where s is the cluster size, N is the total number of lattice sites, and the sum runs over all clusters excluding the largest one. The variable M_2 at R_c as a function of the system size is shown in the inset of Fig. 6(a), where another scaling behavior is observed consistent with $M_2 \sim L^{\frac{\gamma}{\nu}}$, with $\frac{\gamma}{\nu} = 1.80 \pm 0.02$, in agreement with the scaling relation $\frac{\gamma}{\nu} = 2D_f - d$.

We measured the correlation function, also known as the connectivity correlation function, defined as

$$g(r) = \langle \delta_{ij} \rangle - \frac{s_{\max}^2}{N^2}, \tag{34}$$

where δ_{ij} is 1 if both site i and site j are occupied by the same cluster and 0 otherwise, and $s_{\max}$ is the size of the largest cluster. Figure 6(b) shows that at R_c, both correlation functions are power laws with an exponent consistent with the one for random percolation [34].

B. Substrate with impurities

To account for the presence of impurities (e.g., Pb atoms [35]), quenched impurities are randomly distributed on the substrate. These impurities do not react and remain immobile, influencing only the adsorption, as an occupied site, which promotes the adsorption of monomers.

Since impurities geometrically favor the coverage of monomers, the value of $\theta_m - \theta_d$ as a function of impurity coverage θ_{imp} is plotted in Fig. 7. A maximum is observed at a specific value of the coverage by impurities. The position at which the maximum occurs depends on the ratio R; low values of R favor monomers, leading to an earlier maximum, while a high ratio disfavors monomers, thus shifting the

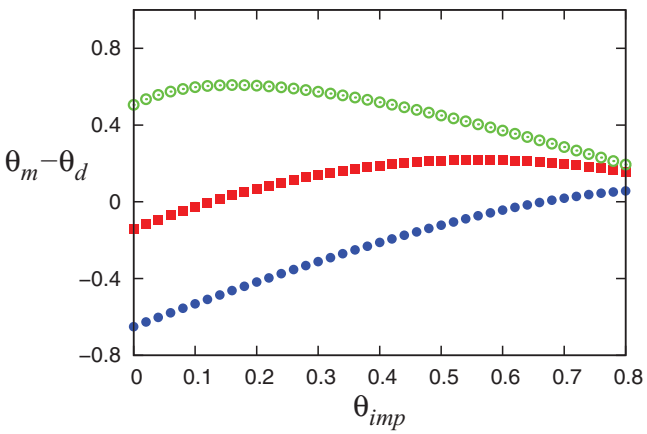

FIG. 7. (Color online) Difference in the jamming coverage of monomers and dimers as a function of the impurity coverage, in two dimensions, for $R = 0.1$ (open circles), $R = 1$ (filled squares), and $R = 10$ (filled circles).

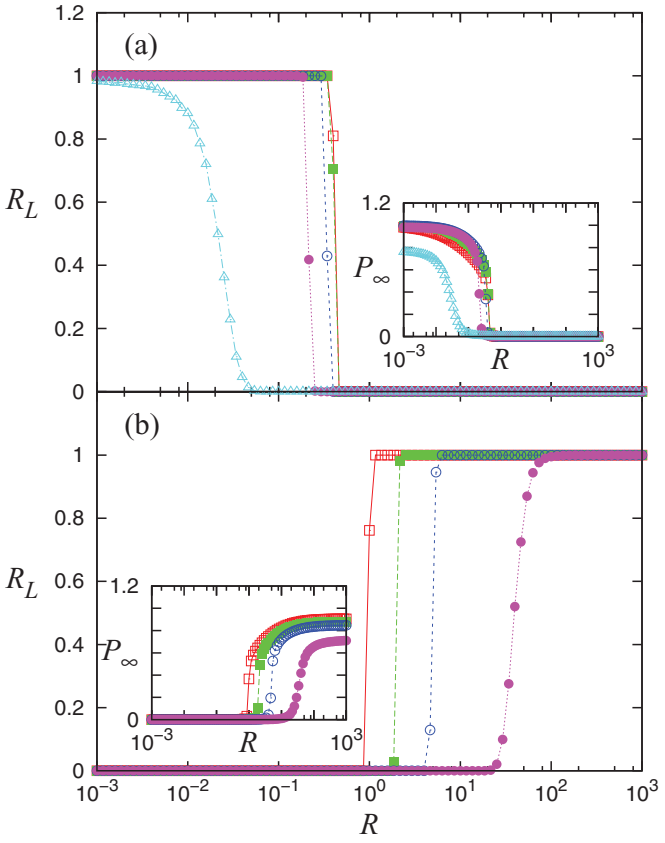

FIG. 8. (Color online) Wrapping probability as a function of the ratio R, in two dimensions, for (a) monomers with impurity coverage, from right to left, of 0%, 10%, 20%, 30% and, 40% and (b) dimers with impurity coverage, from left to right, of 0%, 10%, 20%, and 30%. Simulation of a system size of 512^2. Inset: Fraction of sites belonging to the largest cluster P_∞.

position of the maximum to larger values. These results open up the possibility of tuning the production of monomers by controlling the fraction of impurities.

Additionally, impurities also shift the percolation threshold. Figures 8(a) and 8(b) show the spanning probability R_L as a function of the ratio R for different values of impurities coverage. The monomers percolation transition is mainly affected at larger impurity coverage and is shifted to lower values of R. The dimer percolation transition, on the other hand, is shifted to higher values of R. At higher values of impurity coverage, the clusters of impurities predominate on the surface and neither monomers nor dimers percolate. The insets in Figs. 8(a) and 8(b) show the fraction of sites belonging to the largest cluster P_∞ as a function of R, with $P_\infty = \frac{\langle s_{\max}\rangle}{N(1-\theta_{\text{imp}})}$, where N is the total number of lattice sites, and θ_{imp} is the coverage of impurities. In the case of monomers, as disclosed by the behavior of the spanning probability, the size of the largest cluster is only significantly affected by impurities for values of impurity coverage above 30%. In the case of dimers, impurities have a larger effect on R_L and P_∞.

VI. FINAL REMARKS

We introduced a model based on the RSA of monomers and dimers, representing acetyl and cleaved products, respectively, in the low desorption limit. The kinetic rules based on recent results by Wang and Liu are dependent on the local configuration provided by the neighboring adsorbed sites instead of configuration-independent rates.

The properties of the model were studied in a one-dimensional lattice and also extended to a two-dimensional square lattice. In the latter case, the model describes the mechanisms of ethanol electro-oxidation on a Pt(100) surface, suggested by Wang and Liu [2]. In one dimension, we have analytically solved the model in three cases: the same deposition rate for dimer and monomer adsorption, preferential dimer site adsorption, and different deposition rates. MC simulations are in agreement with the analytical solution. In two dimensions we have studied the jammed state and percolation transition through MC simulations. The percolation properties of the adsorbed species reveal that, while monomers percolate at low ratios of dimer/monomer deposition rate, dimers percolate at high ratios. The influence of impurities has also been monitored, disclosing that the coverage of monomers is significantly improved by their presence.

In the present work, we have restricted ourselves to study of a system as simplified as proposed in Sec. I. One can clearly devise extensions of the basic model to include desorption and reaction pathways not included in the present paper. Molecular dynamics studies could, in principle, provide a more complete picture of the particle arrangements on the surface, but at a shorter time scale. It would certainly be interesting to study the atomistic mechanisms based on cooperative thermal effects, which could affect some of the reaction pathways.

ACKNOWLEDGMENTS

The authors are grateful for support through Fundacão para a Ciência e a Tecnologia fellowships (CD SFRH/BD/31833/2006, AC SFRH/BPD/3475/2007) and the warm hospitality of the T-1 group at Los Alamos National Laboratory (LANL). Work at LANL was supported by the US Department of Energy (US DOE). LANL is operated by Los Alamos National Security, LLC, for National Nuclear Security Administration of US DOE under Contract No. DE-AC52-06NA25396. A.C. acknowledges useful comments by Neil Henson in the early stages of this work.

[1] H. Wang, Z. Jusys, and R. J. Behm, J. Phys. Chem. B **108**, 19413 (2004).
[2] H.-F. Wang and Z.-P. Liu, J. Am. Chem. Soc. **130**, 10996 (2008).
[3] H.-F. Wang and Z.-P. Liu, J. Phys. Chem. C **111**, 12157 (2007).
[4] P. Parpot, N. Nunes, and A. P. Bettencourt, J. Electroanal. Chem. **596**, 65 (2006).

[5] J. W. Evans, Rev. Mod. Phys. **65**, 1281 (1993).
[6] A. Cadilhe, N. A. M. Araújo, and V. Privman, J. Phys. Condens. Matter **19**, 065124 (2007).
[7] N. A. M. Araújo and A. Cadilhe, Phys. Rev. E **73**, 051602 (2006).
[8] N. A. M. Araújo and A. Cadilhe, J. Stat. Mech. (2010) P02019.
[9] B. Bonnier, Phys. Rev. E **64**, 066111 (2001).
[10] B. Bonnier, M. Hontebeyrie, Y. Leroyer, C. Meyers, and E. Pommiers, Phys. Rev. E **49**, 305 (1994).
[11] V. Privman, Trends Stat. Phys. **1**, 89 (1994).
[12] B. J. Brosilow, R. M. Ziff, and R. D. Vigil, Phys. Rev. A **43**, 631 (1991).
[13] J. Feder, J. Theor. Biol. **87**, 237 (1980).
[14] N. Araújo, *Nonequilibrium Thin-Film Growth: Kinetics of Deposition and Post Evolution Relaxation* (Lambert Academic, Saarbrücken, Germany, 2010).
[15] J. W. Evans and R. S. Nord, Phys. Rev. B **31**, 1759 (1985).
[16] R. H. López, F. Romá, V. Gargiulo, J. L. Sales, and G. Zgrablich, J. Phys. Chem. B **112**, 8619 (2008).
[17] J. J. González, P. C. Hemmer, and J. S. Høye, Chem. Phys. **3**, 228 (1974).
[18] P. J. Flory, J. Am. Chem. Soc. **61**, 1518 (1939).
[19] A. S. McLeod and L. F. Gladden, J. Chem. Phys. **110**, 4000 (1999).
[20] L. Finegold and J. T. Donnell, Nature **278**, 443 (1979).
[21] J. Feder and I. Giaever, J. Colloid Interface Sci. **78**, 144 (1980).
[22] G. Y. Onoda and E. G. Liniger, Phys. Rev. A **33**, 715 (1986).
[23] A. J. Ramirez-Pastor, J. L. Riccardo, and V. Pereyra, Langmuir **16**, 682 (2000).
[24] C. Zuppa, M. Ciacera, and G. Zgrablich, Langmuir **15**, 5984 (1999).
[25] D. J. Stacchiola, M. Ciacera, C. Zuppa, T. P. Eggarter, and G. Zgrablich, J. Chem. Phys. **108**, 1730 (1998).
[26] G. Kondrat, J. Chem. Phys. **124**, 054713 (2006).
[27] J. W. Lee, J. Phys. A **29**, 33 (1996).
[28] E. Ben-Naim and P. L. Krapivsky, J. Phys. A **27**, 3575 (1994).
[29] M. J. S. Farias, G. A. Camara, and A. A. Tanaka, J. Solid State Electrochem. **11**, 1465 (2007).
[30] L. R. Lynd, Annu. Rev. Energy Environ. **21**, 403 (1996).
[31] J. W. Evans, in *Nonequilibrium Statistical Mechanics in One Dimension*, edited by V. Privman (Cambridge University Press, Cambridge, 1997).
[32] F. Rampf and E. V. Albano, Phys. Rev. E **66**, 061106 (2002).
[33] J. Hoshen and R. Kopelman, Phys. Rev. B **14**, 3438 (1976).
[34] D. Stauffer and A. Aharony, *Introduction to Percolation Theory* (Taylor & Francis, London, 1994).
[35] N. D. Spencer and G. A. Somorjai, Rep. Prog. Phys. **46**, 1 (1983).